ORIGINAL ARTICLE

Secondary alterations in bone mineralisation and trabecular thickening occur after long-term estrogen deficiency in ovariectomised rat tibiae, which do not coincide with initial rapid bone loss

L. M. O'Sullivan[1] · H. Allison[1] · E. E. Parle[1] · J. Schiavi[1] · L. M. McNamara[1]

Abstract

Summary This study delineates the time sequence of changes in bone tissue mineralisation in ovariectomised rats. We report that changes in bone mineral distribution arise secondary to the initial rapid bone loss but coincide with trabecular thickening. We propose that these changes compensate for elevated stresses in remaining trabeculae after bone resorption.

Introduction Recent studies have shown that osteoporosis is not simply a disease of bone loss and microarchitectural degradation but that important changes in tissue composition also occur. Such changes may be a secondary response to early bone loss, but the time sequence of changes in bone mineral distribution is not fully understood. The objective of this study was to quantify the temporal effects of estrogen deficiency on trabecular mineral distribution in the tibia of ovariectomised (OVX) rats.

Methods Weekly in vivo micro-CT scans and morphometric and bone mineral density distribution analyses of the proximal tibia were conducted for the first 4 weeks of estrogen deficiency and then at 8, 14 and 34 weeks.

Results Here we report that although trabecular bone volume and architecture are significantly deteriorated within the first 4 weeks of estrogen deficiency, there is no change in the distribution of bone mineral within trabeculae during this initial period. The rate of bone loss in OVX animals dramatically reduced between week 4 and week 14, which coincided with the initiation of increases in trabecular thickness and mineralisation in the OVX group.

Conclusions Together this study reveals for the first time that alterations in bone mineralisation and trabecular thickening arise secondary to the initial rapid bone loss. We propose that these secondary mineralisation changes act to reinforce the trabecular network in an attempt to compensate for the increased loading that ensues after severe bone loss. This study provides an insight into temporal changes in bone mineral distribution in estrogen deficiency.

Keywords In vivo micro-CT · Mineral heterogeneity · Osteoporosis · Ovariectomised rat model · Trabecular morphology

Introduction

Osteoporosis is a metabolic skeletal disorder, which is characterised by an imbalance in the natural bone remodelling

✉ L. M. McNamara
laoise.mcnamara@nuigalway.ie

1 Mechanobiology and Medical Devices Research Group (MMDRG), Centre for Biomechanics Research (BioMEC), Biomedical Engineering, College of Engineering and Informatics, National University of Ireland Galway, Galway, Ireland

cycle resulting in severe bone loss. The fundamental concern with the disease of osteoporosis is that the mechanical strength of the bone is compromised to such a degree that bone fractures occur under loading conditions not associated with fracture in healthy bones. The overall mechanical strength of bone is determined by bone mass, a quantitative measure of the total bone in a specific area of interest, and bone quality, encompassing bone tissue microarchitecture, composition and the degree of microdamage. The contribution of each of these parameters to fracture susceptibility in estrogen deficiency has been investigated to varying degrees.

Estrogen deficiency in postmenopausal women is typically associated with reductions in bone volume and trabecular structure [1–3]. Micro-computed tomography (micro-CT)

and histomorphometry analyses of bone tissue from estrogen-deficient animal post-mortem have revealed that rapid bone loss in early estrogen deficiency occurs by means of removal of whole trabecular elements [4], severing of trabecular struts [3], but not trabecular thinning [5]. In vivo micro-CT studies allow for repeated assessment of bone loss in estrogen-deficient animals. Using such approaches it has been reported that trabecular bone volume and microarchitecture are rapidly depleted within the first month of estrogen deficiency in ovariectomised rats [6–9], but studies conflict with regard to whether this occurred by means of trabecular thinning [7, 9] or targeted removal of entire trabecular struts [6, 8]. Most interestingly, it was reported that trabecular thickening occurs at later stages of estrogen deficiency [6–8]. On this basis, it was proposed that osteoporosis was a disease of accelerated bone metabolism and that mechanical adaptation plays a role in trabecular thickening.

Recent studies have shown that osteoporosis is not simply a disease of bone loss and microarchitectural degradation but that important changes in tissue composition also occur. In a study of quantitative backscattered imaging (qBEI) of human osteoporotic bone tissue, the mineral content and heterogeneity of mineral distribution increased in individual trabeculae, which was also shown to render the tissue more brittle through mechanical testing [10]. In animal models of osteoporosis, tissue-level mineral distribution is altered [11], and changes in mineralised crystal maturity, mineral-to-matrix ratio and collagen cross-linking occur [12]. In particular quantitative backscattered imaging (qBEI) of trabeculae of ovine femurs revealed that bone tissue mineral distribution became more heterogeneous in estrogen-deficient animals, when compared to controls, and these changes were dependent on the anatomical region and the age of the animal [13]. However, qBEI and ex-vivo micro-CT studies on trabecular bone from the femur and vertebra of estrogen-deficient rats have reported no change in mean mineral density [14–16] and a minimal reduction of mineral heterogeneity [15] late in estrogen deficiency. However, these studies focused on bone tissue post-mortem and could not capture longitudinal changes in mineral heterogeneity during estrogen deficiency.

Recently a technique was developed to quantify local mechanical environment of osteocytes and osteoblasts from healthy and osteoporotic bone in a rat model of osteoporosis. Using this approach it was reported that the mechanical environment of osteoblasts and osteocytes is altered in the initial estrogen deficiency (4 weeks) but restored at later stages (34 weeks). On this basis it was proposed that mechanobiological responses are activated by osteocytes to restore their local mechanical environment after it has been perturbed by bone loss due to ovariectomy [17]. The putative mechanisms by which this occurs were proposed to be either secondary changes in bone mineral distribution [13] or increased trabecular thickness [8]. However, to date no study has conducted a comprehensive and temporal in vivo analysis of the changes in bone mineral distribution and microarchitecture in estrogen-deficient animals, and thus the relationship between changes in bone mineral distribution and microarchitecture is not yet fully understood.

The objective of this study was to use in vivo μCT to conduct a comprehensive analysis of the temporal effects of estrogen deficiency on the trabecular bone mineral distribution in the proximal tibia of an ovariectomised rat model and relate these changes to the time sequence of changes in bone loss and trabecular microarchitecture.

Materials and methods

Animal model

Female retired breeder Wistar rats (6-month old, Charles River, Ireland) were assigned randomly to groups for either (a) bilaterally ovariectomy (OVX, $n = 10$) or (b) a sham operation (SHAM, $n = 9$) by the vet conducting the surgeries. Then the animals were assigned to longitudinal studies of either initial phase of estrogen deficiency (OVX, $n = 5$, SHAM, $n = 5$) or a longitudinal study of the long-term effects of estrogen deficiency (OVX, $n = 5$, SHAM, $n = 5$), as is described further below. Success of ovariectomy was confirmed in necropsy by the absence of ovaries and determining atrophy of the uterine horns. All animal work was carried out under license from the Animal Care and Research Ethics Committee (ACREC) of the National University of Ireland Galway and the Health Products Regulatory Authority (HPRA), the national authority for scientific animal protection in Ireland. These OVX and SHAM surgery groups were either (1) followed by weekly in vivo micro-CT scanning to investigate initial changes in morphometry and mineralisation due to estrogen deficiency by scanning at day 0, week 1, week 2, week 3 and week 4 (OVX $n = 5$, SHAM $n = 5$), after which they were sacrificed at 4 weeks post-ovariectomy (body weight, OVX: 410 ± 68 g, SHAM: 445 ± 21 g, mean $\pm$ standard deviation) or (2) followed to investigate changes in morphometry and mineralisation in long-term estrogen deficiency by scanning at day 0, week 4, week 8 and week 34 (OVX $n = 5$, SHAM $n = 5$) and were sacrificed at 34 weeks post-ovariectomy (body weight, OVX: 361 ± 25 g, SHAM: 423 ± 41 g, mean $\pm$ standard deviation). The in vivo micro-CT procedures and analysis, which are described in further detail below, were identical for initial and long-term estrogen deficiency studies, unless otherwise stated. One SHAM animal in the long-term study died at week 29 as a result of tumours related to ageing; therefore scans from this animal were excluded from all analysis, reducing the long-term SHAM group to four animals.

In vivo micro-CT scanning

At each time point, the right tibia of each animal was scanned with an isotropic resolution of 15 μm, using an in vivo micro-CT system (VivaCT40, Scanco Medical AG, Bassersdorf, Switzerland). The following scan settings were used: X-ray tube potential of 70kVp, current 114 μA, integration time 300 ms and 1000 projections per 180°, and a 0.5 mm thick aluminium filter was used to reduce beam hardening artefacts. During the procedure, the animals were kept under isoflurane, and their respiratory rate was monitored throughout. The right hind limb was positioned and fixed in a cylindrical fixture, such that it was the only radiated region during the scan. Each scan lasted approximately 20 min and emitted close to 850 mGy on the scanned area. This ionisation is not expected to affect the bone structure, as a previous study reported no bone structural effect for 8 weekly scans at the proximal tibia of a rat when doses up to 939 mGy were administered [18]. Weekly calibration quality checks were conducted scanning a phantom containing five rods of varying known mineral densities (0, 100, 200, 400 and 800 mgHA/ccm). All quality control checks during this study indicated that the accuracy of density measurements was within the recommended range provided by the manufacturer to denote satisfactory instrument calibration.

A region of interest was chosen, which comprised of a 3 mm section of metaphyseal trabecular bone directly below the growth plate in the proximal tibia. The end of the growth plate was recognised by the last micro-CT image containing an intact chondrocyte seam. The next scan distal to the chondrocyte seam was the start point for the metaphyseal volume of interest (VOI). The VOIs were defined with a semiautomated segmentation process, whereby the user defined 2D borders around the trabecular network for specific images from the image series, which were then extrapolated across all intervening images using a dynamic interpolation algorithm in the Scanco segmentation software. Slice matching was used to ensure identical VOIs were analysed for baseline and follow-up images of each animal. This involved using the first and last μCT image of each baseline scan VOI to identify the appropriate limits for follow-up scans, while also keeping the slice number constant for every analysis. The presence of bone in the micro-CT scans was separated from the other components present in the sample (i.e. air and marrow) using a global threshold value of 614 mg HA/ccm, following guidelines outlined in [12, 19].

Morphometric analysis

A series of microarchitectural parameters were quantified from the three-dimensional reconstruction of the trabecular volume of interest, using evaluation scripts in the Scanco Image Processing Language (IPL). These parameters allow

for detailed comparison between the trabecular structure of the estrogen-deficient (OVX) and healthy (SHAM) animals at each time point. Bone volume fraction (BV/TV) and 3D trabecular thickness (Tb.Th [mm]) were quantified to describe the bone mass and its distribution. Structural model index (SMI), connectivity density of the trabecular network (Conn.D [mm^{-3}]) and the degree of anisotropy in the strut network (DA), Trabecular number (Tb.N [mm^{-1}]) and trabecular separation (Tb.Sp [mm]) were analysed to complete a detailed description of the trabecular structure in the proximal tibia of the OVX and SHAM groups.

Bone mineral density distribution analysis

Bone mineral density distribution analysis has been used to assess the changes in bone composition during estrogen deficiency. The method allows for assessment of the amount of bone volume at various stages of mineralisation in order to give a detailed description of the bone quality. The raw micro-CT data files were quantitatively processed to create bone mineral density distribution (BMDD) measurements for each trabecular data set. Grey level histograms were produced from the micro-CT images to show the frequency of occurrence of voxels at a certain grey level or tissue mineral density (mg HA/ccm); see example curve in Fig. 1D. To prevent partial volume effects from causing an underestimation of the trabecular bone mineral density, the surface voxels (one layer) from each trabecula are excluded from these histograms. A custom python script was used to characterise specific characteristics of each distribution: weighted mean tissue mineral density (mean mineral density, mgHA/ccm), the most frequent mineral density (mode mineral density, mgHA/ccm), the full width at half maximum of the mineral distribution curve (mineral heterogeneity, mgHA/ccm) [20] and the bone volume at low, medium or high mineral densities. The bone volume (mm^3) at low mineral density (low mineral BV, mm^3) was quantified below the 25th percentile mineral density value of the baseline BMDD curves, whereas high mineral density bone (high mineral BV, mm^3) was above the 75th percentile value of the baseline BMDD curves, and medium mineral BV (mm^3) was the volume of bone between these limits (Supp. Table 1). This BMDD analysis approach allows for a comprehensive and quantitative description of changes in the mineral composition of trabecular bone from the proximal tibia due to estrogen deficiency (OVX vs SHAM).

Statistics

All parameters (BV/TV, Conn.D, Tb.N, Tb.Th, Tb.Sp, DA, SMI, mean mineral density, mode mineral density, mineral heterogeneity, low mineral BV, medium mineral BV and high
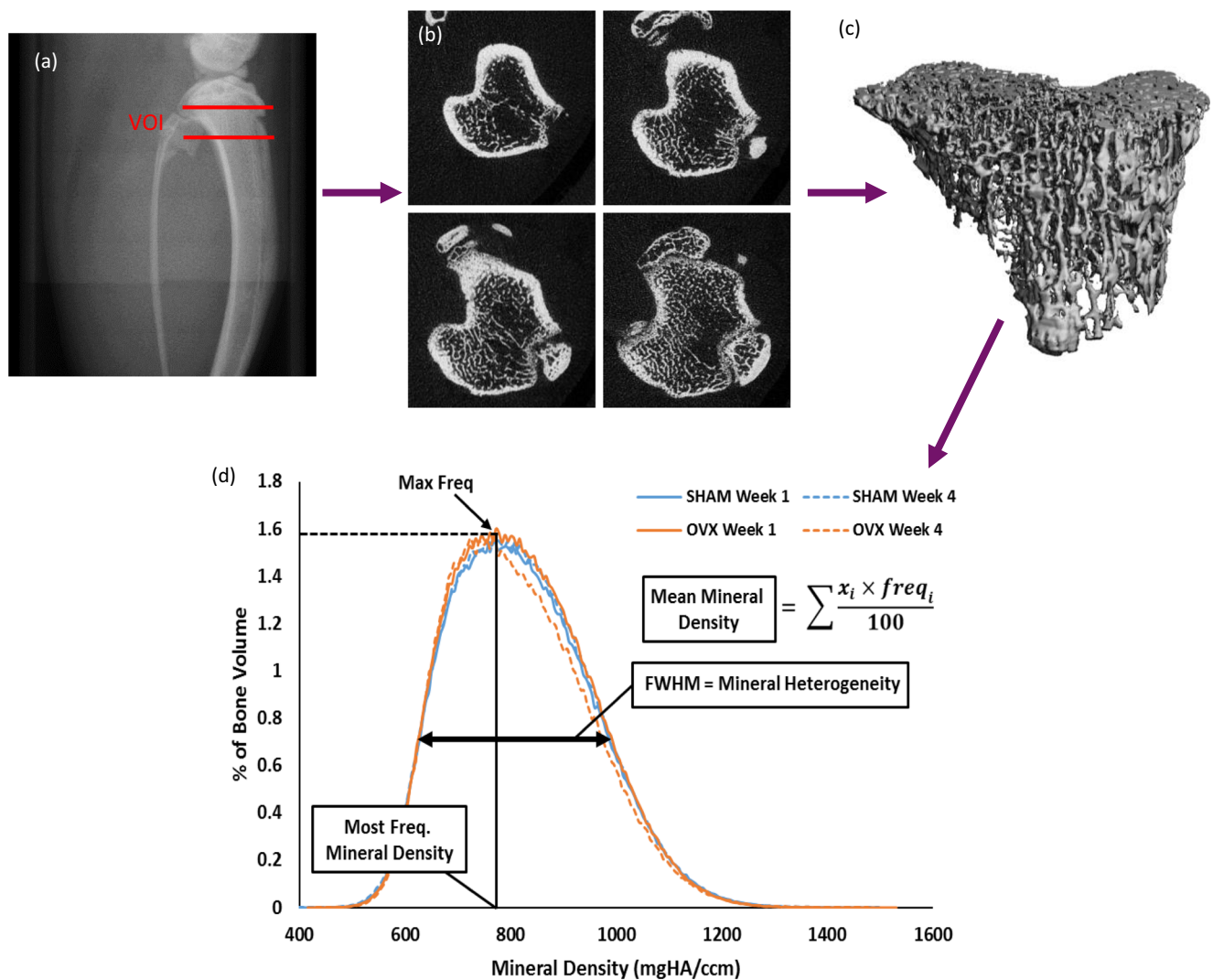
Fig. 1 Sequence of in vivo micro-CT scan depicting (A) the scout view of rat proximal tibia which is used to specify VOI for micro-CT scan; (B) a sample of the micro-CT image series produced for the chosen VOI in the proximal tibia; (C) the 3D reconstruction of the metaphyseal trabecular bone in the proximal tibia, which is created by segmenting and thresholding the micro-CT image series and is used for morphological and mineralisation analysis; and (D) bone mineral density distribution plot (BMDD) with notations for the parameters used to compare plots from OVX and SHAM groups

mineral BV) were tested for normal distribution using the Kolmogorov-Smirnov normality test. Student t-tests were used to analyse the statistical significance of the differences between the OVX and age-matched control (SHAM) groups at each time point, for parameters which passed the normality test. For parameters which failed the normality test (initial phase study: mean mineral density, mode mineral density and high mineral BV and long-term study: Conn.D, Tb.N, Tb.Sp and mean mineral density), a nonparametric Mann-Whitney rank sum test was used to compare OVX and SHAM animals at each time point. A p value of < 0.05 was considered significant.

For all parameters of interest (BV/TV, Conn.D, Tb.N, Tb.Th, Tb.Sp, DA, SMI, mean mineral density, mode mineral density, mineral heterogeneity, low mineral BV, medium mineral BV and high mineral BV), the main effects of time and the interaction between time and group (group: OVX or SHAM) were tested using a repeated measures (RM) two-way ANOVA in GraphPad Prism. The effect of time indicates whether the treatment (OVX or normal ageing) changed the parameter over the course of the study, while the interaction between time and group indicates whether the effect of time was different for the two groups. For each parameter where the two-way ANOVA indicated a significant interaction between the time and group effects, Tukey's post hoc multiple comparison tests were performed to detect the differences between the parameter values at the different time points within a single group (OVX or SHAM).

Results

Initial changes in trabecular bone volume and architecture after estrogen deficiency

We analysed initial changes in morphometry due to estrogen deficiency by weekly in vivo micro-CT scanning in the first 4 weeks after ovariectomy and by comparing the change in each parameter relative to the baseline (day 0) values.

BV/TV in the OVX trabecular bone was lower than SHAM by week 1 ($p < 0.01$), week 2 ($p < 0.01$), week 3 ($p < 0.01$) and week 4 ($p < 0.01$) (Fig. 2B). Moreover, Tb.N was lower at week 4 ($p < 0.05$) and Tb.Sp was higher at week 3 ($p < 0.05$)

and week 4 ($p < 0.05$) in the OVX group (Fig. 2C, D). However, there was no difference in Tb.Th between OVX and SHAM groups over the first 4 weeks, (Fig. 2E). These were accompanied by differences between the OVX and SHAM groups in Conn.D, DA and SMI (Supp. Fig. 1).

There were no longitudinal changes in any morphological parameter of the SHAM group over the 4 weeks (Fig. 2). BV/TV, in the OVX group, was reduced at week 1 ($p < 0.01$), week 2 ($p < 0.001$), week 3 ($p < 0.0001$) and week 4 ($p < 0.0001$) when compared to the baseline (Fig. 2B). Tb.N was reduced in the OVX group at week 2 ($p < 0.05$), week 3 ($p < 0.001$) and week 4 ($p < 0.0001$) compared to baseline (Fig. 2C). Tb.Sp increased in the OVX group between week 2,
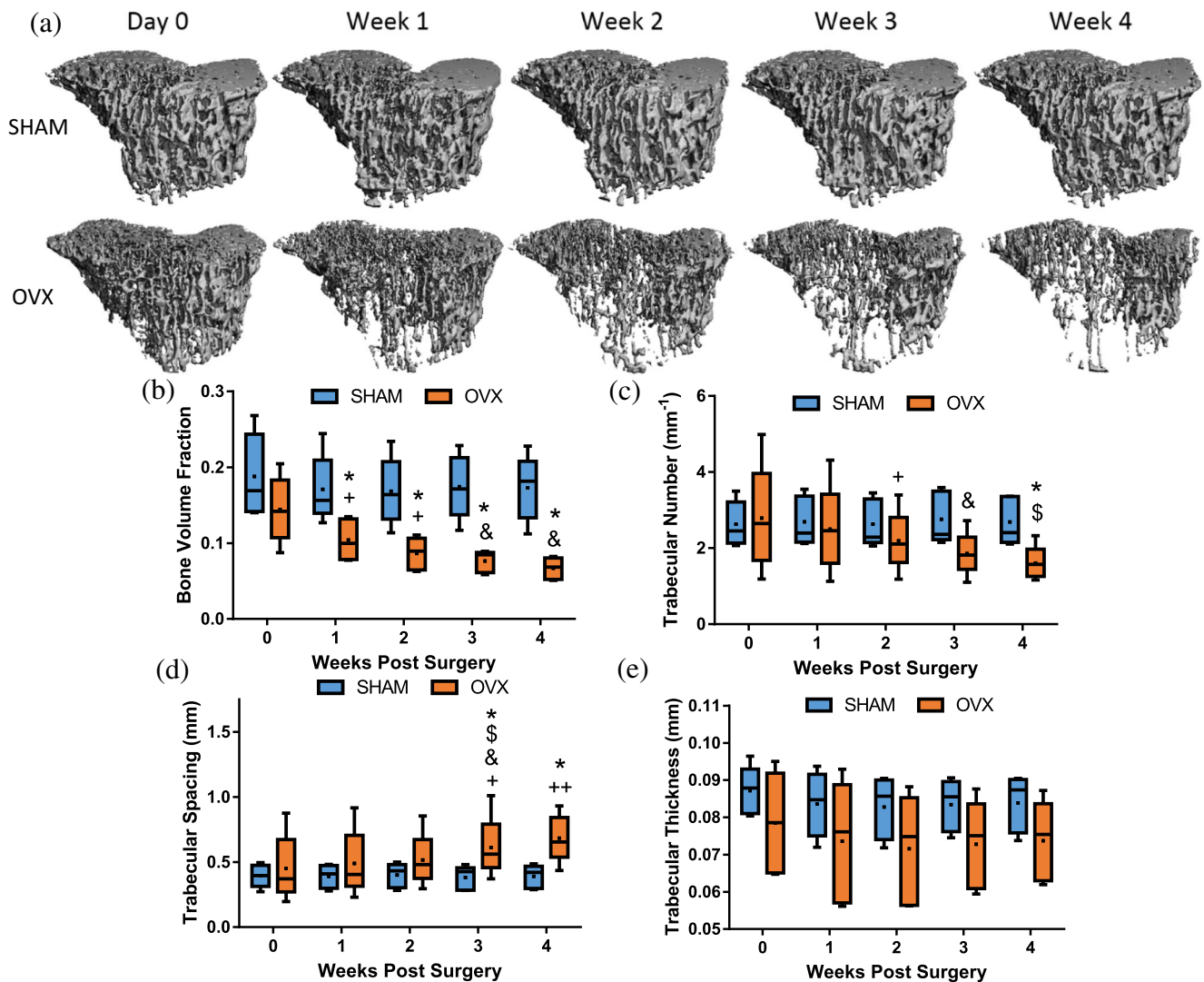

Fig. 2 (A) 3D micro-CT images of metaphyseal trabecular bone in the proximal tibia of one SHAM and one OVX animal during initial phase of estrogen deficiency. (B)–(E) Longitudinal comparison of microarchitectural parameters in SHAM and OVX animals during initial phase of estrogen deficiency. Number of animals per group: day 0–week 4 ($n = 5$). Box plots and whiskers display the following: whiskers extend between min and max values of data set, the box extends from 25th to 75th percentiles, horizontal line across the box is the median value and the black dot represents the mean of the data. $p < 0.05$ was considered significant. '*' indicates a significant difference between SHAM and OVX animals at the same time point. All remaining symbols indicate significant longitudinal differences within the same group: '+' indicates significance compared to baseline value (day 0), '&' indicates significance compared to week 1, '$' indicates significance compared to week 2, '£' indicates significance compared to week 3 and '++' indicates significance compared to all previous time points

week 3 and week 4 ($p < 0.0001$) (Fig. 2D). These were also accompanied by longitudinal changes in Conn.D, DA and SMI in the OVX animals (Supp. Fig. 1). The RM two-way ANOVA indicated that the time effect on BV/TV, Conn.D, Tb.N, Tb.Sp, DA and SMI was significantly different between OVX and SHAM groups. However, there was no difference for Tb.Th up to week 4.

Bone mineral distribution is not altered in the initial phase of estrogen deficiency

We analysed initial changes in mineralisation due to estrogen deficiency in the first 4 weeks after ovariectomy. The tissue volume (mm^3) at low mineral density in the OVX group was significantly lower than SHAM at week 2 ($p < 0.05$), week 3 ($p < 0.01$) and week 4 ($p < 0.01$) (Fig. 3D). Moreover, tissue volume (mm^3) at medium mineral density was lower at week 1 ($p < 0.05$), week 2 ($p < 0.05$), week 3 ($p < 0.01$) and week 4 ($p < 0.01$) in the OVX group, and tissue volume (mm^3) at high mineral density was lower at week 3 ($p < 0.01$) and week 4 ($p < 0.01$) (Fig. 3D, E, F). Despite changes in bone volume by week 1, there was no difference in the bone mineral density distribution over the first 4 weeks in the OVX or SHAM groups, as indicated by the statistical comparisons between OVX and SHAM of mean mineral density (813.42 ± 12.49 vs 799.93 ± 25.88 mgHA/ccm, $p = 0.33$), mode mineral

density (754.443 ± 13.92 vs 746.48 ± 42.92 mgHA/ccm, $p = 0.70$) and mineral heterogeneity (331.32 ± 22.80 vs 289.86 ± 51.55 mgHA/ccm, $p = 0.14$) at week 4 (Fig. 3).

There was no longitudinal change in the tissue volume (mm^3) at any mineral density in the SHAM group over the 4 weeks, (Figs. 3 and 5D, E, F). The tissue volume at low, medium and high mineral BV was reduced in the OVX group at week 1 ($p < 0.05$, $p < 0.01$, $p < 0.01$), week 2 ($p < 0.01$, $p < 0.0001$, $p < 0.0001$), week 3 ($p < 0.0001$) and week 4 ($p < 0.0001$) compared to baseline (Fig. 3D, E, F).

The RM two-way ANOVA indicated that the time effect on low, medium and high mineral BV was significantly different between OVX and SHAM groups. However, there was no difference for mean mineral density, mode mineral density and mineral heterogeneity up to week 4 (Fig. 3).

Bone loss in long-term estrogen deficiency

We analysed long-term changes in morphometry due to estrogen deficiency by in vivo micro-CT scanning at day 0, week 4, week 8, week 14, and week 34 after ovariectomy and by comparing the change in each parameter relative to the day 0 baseline values.

BV/TV in the OVX trabecular bone was lower than SHAM at week 4, week 8, week 14 and week 34 ($p < 0.001$) (Fig. 4B). Tb.N in the OVX group was lower compared to the SHAM
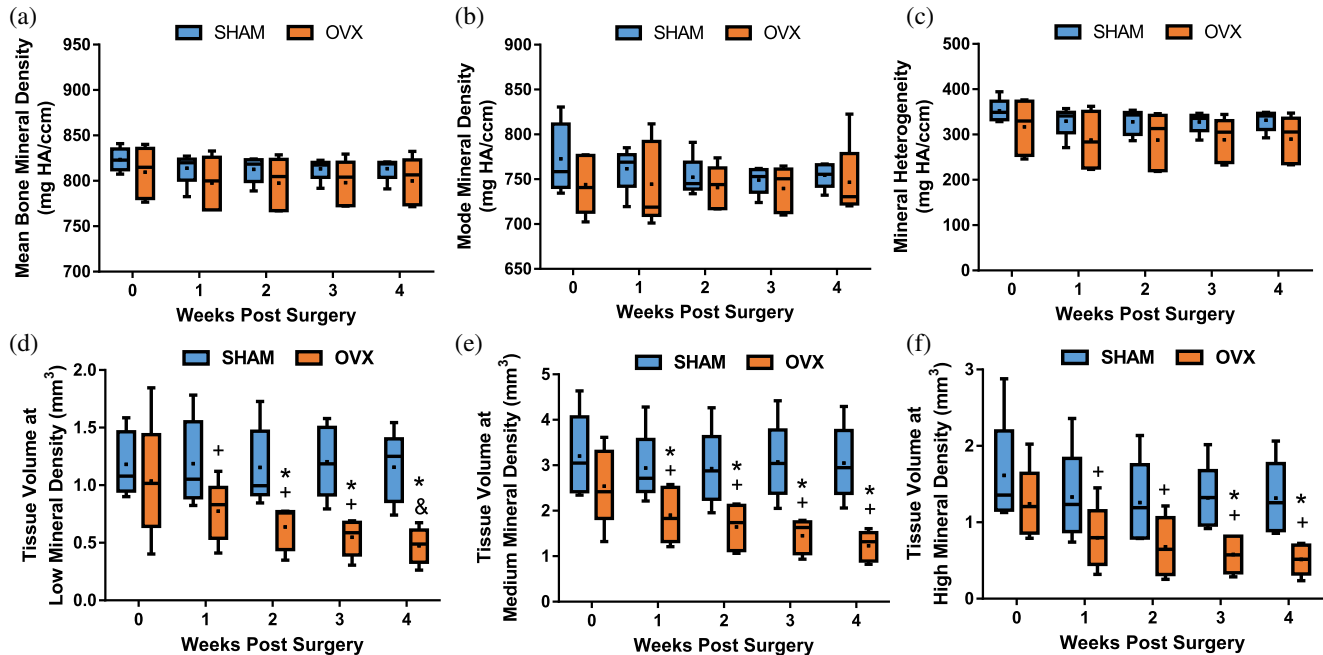

Fig. 3 (A)–(F) Longitudinal comparison of bone mineral density distribution (BMDD) parameters in SHAM and OVX animals during initial phase of estrogen deficiency. Number of animals per group: day 0–week 4 ($n = 5$). Box plots and whiskers display the following: whiskers extend between min and max values of data set, the box extends from 25th to 75th percentiles, horizontal line across the box is the median value and the black dot represents the mean of the data. $p < 0.05$ was considered significant. '*' indicates a significant difference between SHAM and OVX animals at the same time point. All remaining symbols indicate significant longitudinal differences within the same group: '+' indicates significance compared to baseline value (day 0), '&' indicates significance compared to week 1, '$' indicates significance compared to week 2, '£' indicates significance compared to week 3 and '++' indicates significance compared to all previous time points
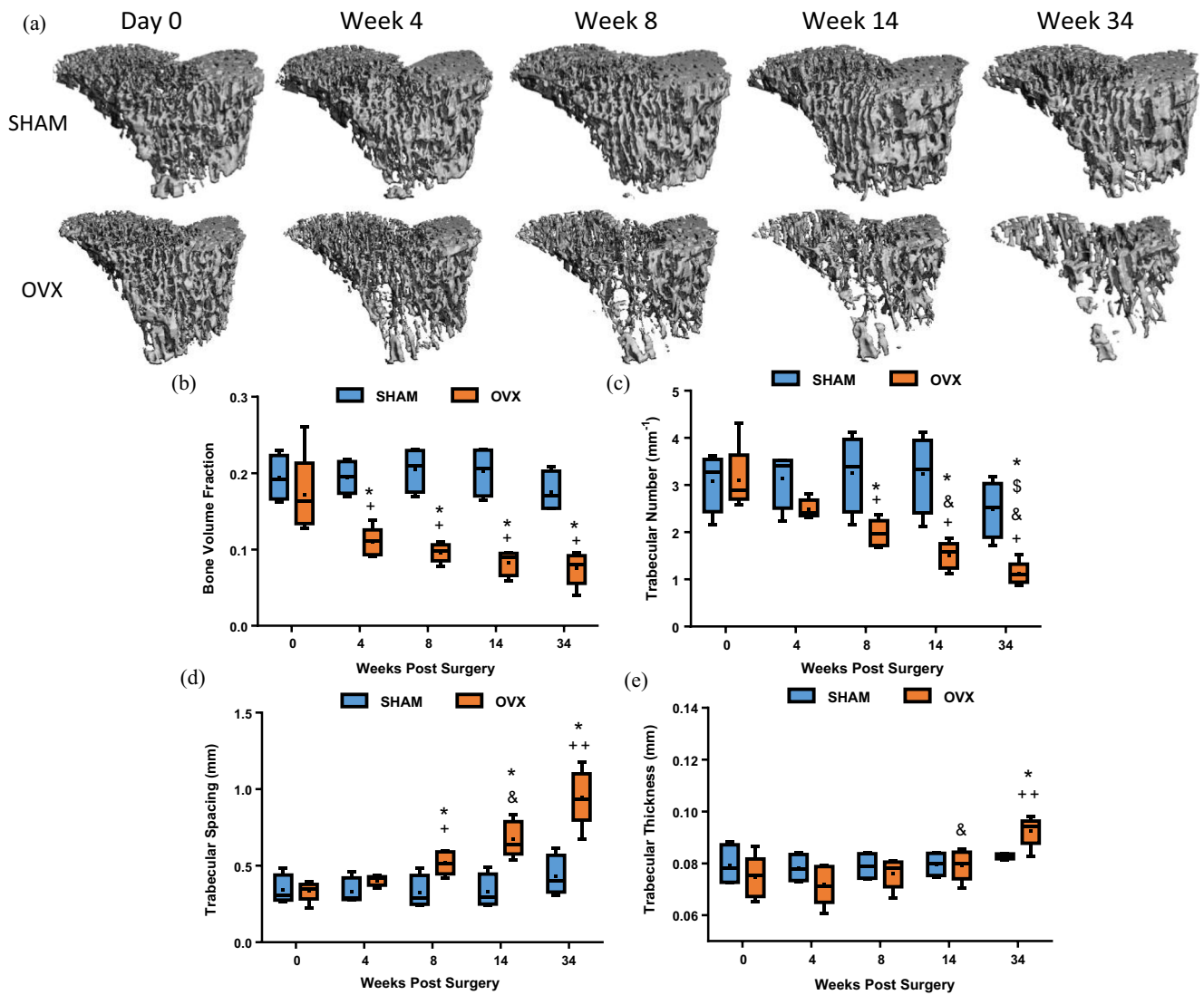
Fig. 4 (A) 3D micro-CT images of metaphyseal trabecular bone in the proximal tibia of one SHAM and one OVX animals during long-term estrogen deficiency. (B)–(E) Longitudinal comparison of microarchitectural parameters in SHAM and OVX animals during long-term estrogen deficiency. Number of animals per group: day 0–week 34 (OVX n = 5, SHAM n = 4). Box plots and whiskers display the following: whiskers extend between min and max values of data set, the box extends from 25th to 75th percentiles, horizontal line across the box is the median value and the black dot represents the mean of the data. $p < 0.05$ was

considered significant. '*' indicates a significant difference between SHAM and OVX animals at the same time point. All remaining symbols indicate significant longitudinal differences within the same group: '+' indicates significance compared to baseline value (day 0), '&' indicates significance compared to week 4, '$' indicates significance compared to week 8, '£' indicates significance compared to week 14 and '++' indicates significance compared to all previous time points

group at week 8 ($p < 0.05$), week 14 ($p < 0.05$) and week 34 ($p < 0.01$) (Fig. 4C). Tb.Sp in the OVX group was higher that the SHAM group at week 8 ($p < 0.05$) week 14 and 34 ($p < 0.01$) (Fig. 4D). Tb.Th of the OVX group was significantly higher in the OVX group compared to the SHAM group by 34 weeks post-ovariectomy ($p < 0.05$) (Fig. 4E). These were accompanied by differences between OVX and SHAM in Conn.D and SMI (Supp. Fig. 2).

Tb.N and Conn.D were significantly reduced in the SHAM group by week 34 ($p < 0.05$ and $p < 0.01$, respectively). There were no other longitudinal changes in morphological

parameters in the SHAM group over the 34 weeks. In the OVX group, BV/TV had decreased significantly between day 0 and week 4 ($p < 0.0001$), and after this BV/TV did not change significantly between week 4 and week 34 (Fig. 4B). Tb.N was decreased in the OVX group at week 4 compared to baseline ($p = 0.06$); this decrease was significant at week 8, week 14 and week 34 ($p < 0.01$) (Fig. 4C). Tb.Sp was significantly increased in the OVX group by week 8 compared to baseline ($p < 0.01$) and continued to increase between each time point up to week 34 ($p < 0.05$, $p < 0.0001$) (Fig. 4D). Tb.Th in the OVX group did not change between day 0 and

week 4 but was increased compared to the week 4 value by week 8 ($p = 0.08$), week 14 ($p < 0.001$) and week 34 ($p < 0.0001$) (Fig. 4E). These were accompanied by longitudinal changes in Conn.D and SMI in the OVX group (Supp. Fig. 2). The RM two-way ANOVA indicated that the time effect on BV/TV, Conn.D, Tb.N, Tb.Th, Tb.Sp, DA and SMI was significantly different between OVX and SHAM groups.

Bone mineral distribution is significantly altered in long-term estrogen deficiency

We analysed long-term changes in mineralisation due to estrogen deficiency at day 0, week 4, week 8, week 14, and week 34 after ovariectomy.

The tissue volume (mm^3) at low mineral BV, medium mineral BV and high mineral BV were significantly lower than SHAM at week 4 ($p < 0.0001$, $p < 0.01$, $p < 0.01$), week 8 ($p < 0.0001$), week 14 ($p < 0.0001$) and week 34 ($p < 0.0001$) (Fig. 5D, E, F). Mean mineral density of the OVX group was lower than the SHAM group at week 4 and week 8 ($p = 0.07$ and $p = 0.06$, respectively). Mode mineral density was lower in the OVX group compared to SHAM at week 8 and week 14 ($p = 0.11$ and $p = 0.07$, respectively). Mineral heterogeneity of the OVX group was significantly lower compared to the SHAM animals at week 4, week 8 and week 14 ($p < 0.05$).

However, by week 34 the mean mineral density and mode mineral density of the OVX group were increased compared to the SHAM group ($p = 0.14$ and $p < 0.05$, respectively), and there was no difference in the mineral heterogeneity between the groups (Fig. 5A, B, C).

Bone mineral distribution is altered in long-term estrogen deficiency, but this arises subsequent to the initial rapid phase of bone loss

The RM two-way ANOVA indicated a significant interaction between time and group effects in mean mineral density, mode mineral density, mineral heterogeneity, low mineral BV, medium mineral BV and high mineral BV. There was no longitudinal change in the tissue volume (mm^3) at any specific mineral density level in the SHAM group over the 34 weeks (Fig. 5D, E, F). The tissue volume (mm^3) at low mineral BV and medium mineral BV was reduced in the OVX group at week 4 ($p < 0.05$), week 8 ($p < 0.0001$, $p < 0.01$), week 14 ($p < 0.0001$) and week 34 ($p < 0.0001$) compared to baseline (Fig. 5D, E). The tissue volume (mm^3) at high mineral BV was lower in OVX compared to baseline at week 4 ($p < 0.05$), week 8 ($p < 0.05$, $p < 0.01$) and week 14 ($p < 0.05$), but at week 34, the difference to the baseline was reduced ($p = 0.10$) (Fig. 5F). Mineral heterogeneity was decreased in the OVX
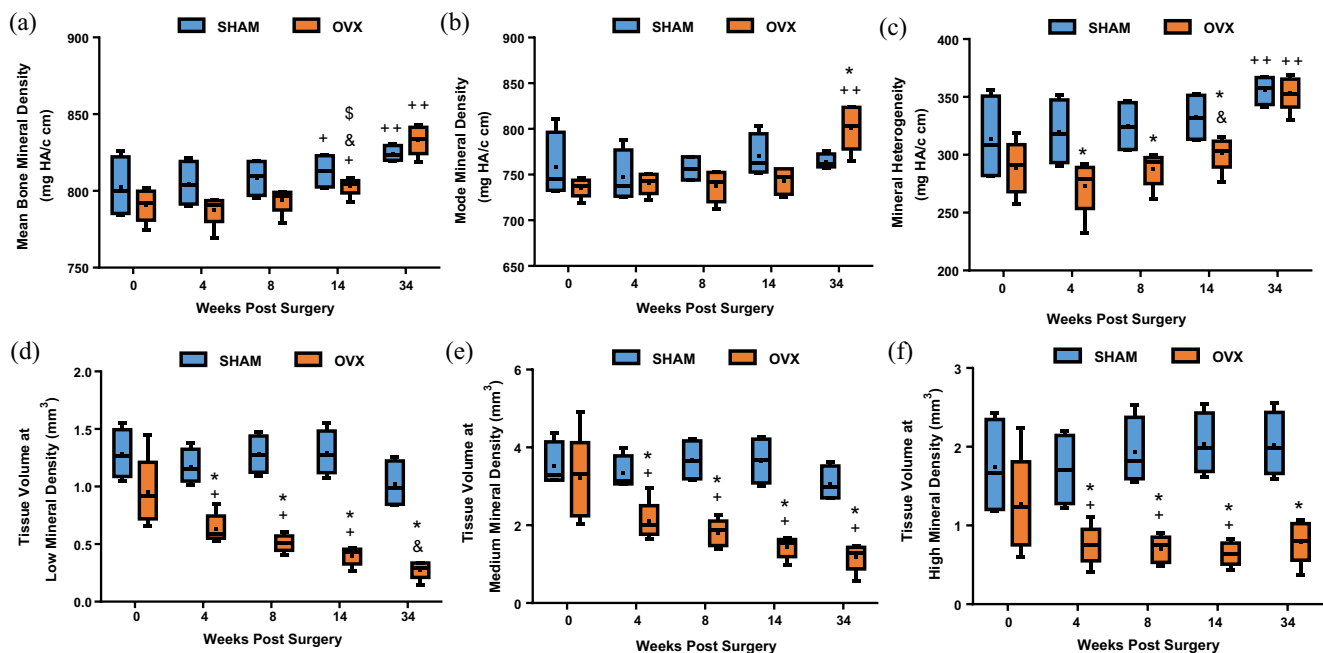

Fig. 5 (A)–(F) Longitudinal comparison of bone mineral density distribution (BMDD) parameters in SHAM and OVX animals during long-term estrogen deficiency. Number of animals per group: day 0–week 34 (OVX n = 5, SHAM n = 4). Box plots and whiskers display the following: whiskers extend between min and max values of data set, the box extends from 25th to 75th percentiles, horizontal line across the box is the median value and the black dot represents the mean of the data. $p < 0.05$ was considered significant. '*' indicates a significant difference between SHAM and OVX animals at the same time point. All remaining symbols indicate significant longitudinal differences within the same group: '+' indicates significance compared to baseline value (day 0), '&' indicates significance compared to week 4, '$' indicates significance compared to week 8, '£' indicates significance compared to week 14 and '++' indicates significance compared to all previous time points

animals at week 4 compared to day 0 ($p = 0.08$) but increased significantly between week 8 and week 34 ($p < 0.01$ and $p < 0.0001$, respectively) (Fig. 5C). Mean mineral density was also significantly increased by week 14 and week 34 ($p < 0.001$) in the OVX animals compared to all previous time points (Fig. 5A). The mean mineral density of the SHAM group was increased by week 14 ($p < 0.05$) and week 34 ($p < 0.0001$), and mineral heterogeneity was increased at week 34 ($p < 0.001$), when compared to day 0 (Fig. 5A, C). These longitudinal changes in the mean mineral density and mineral heterogeneity of the OVX group were exacerbated and occurred at a faster rate than the SHAM group, according to the significant interaction effect from the RM two-way ANOVA of these parameters.

Pearson correlation tests confirmed a significant positive correlation existed between the Tb.Th and all mineral distribution parameters in the OVX animals over the 34-week study (mean mineral density: $R^2 = 0.9947$, $p < 0.001$, mode mineral density: $R^2 = 0.9218$, $p < 0.01$ and mineral heterogeneity: $R^2 = 0.9909$, $p < 0.001$) (Fig. 6). There was no significant correlation between Tb.Th and any of the mineral distribution parameters for the SHAM group (mean mineral density: $R^2 = 0.0069$, $p = 0.998$, mode mineral density: $R^2 = 0.4918$, $p = 0.115$ and mineral heterogeneity: $R^2 = 0.064$, $p = 0.792$).

We conducted an assessment of the skewness and kurtosis of the BMDD curves. The majority of the BMDD curves were practically symmetric (skew value−0.5 and 0.5), while some were moderately skewed (0.65–0.8), whereas the kurtosis for all data was close to a perfect normal distribution (value of 3).

In keeping with our FWHM findings, the skewness did not change within the first 4 weeks after surgery (data not shown) but were significantly altered for the OVX animals at week 34. These results confirm the shifted towards higher mineralisation in later stages of estrogen deficiency (Fig. 5A, B, C). The skewness and kurtosis data are sufficiently close to a normal distribution to validate the use of FWHM as a measurement of the mineral heterogeneity.

Discussion

This study quantified the longitudinal effects of estrogen deficiency on the trabecular microarchitecture and mineral distribution in the tibia of an ovariectomised rat model. Here we report that although a significant reduction in trabecular bone mass and a rapid deterioration of the trabecular structure occur within the first 4 weeks of estrogen deficiency, there was no change in trabecular thickness or tissue mineralisation within this period. Bone loss dramatically reduced between weeks 4 and 14 and reached a homeostasis thereafter up to 34 weeks, which coincided with the initiation of increased bone mineral density, altered mineral distribution and trabecular thickening. Together these results provide the first evidence in uncovering the temporal nature of changes in bone mineral distribution in estrogen deficiency.

There are a number of limitations that need to be considered. Firstly, the estrogen-deficient rat model may differ from the human osteoporosis since there are differences in the biology of rats and human [21]. However, the ovariectomised

Fig. 6 Correlation of trabecular thickness to parameters of bone mineral density distribution in the OVX animals in long-term estrogen deficiency. Scatter plots display the mean ± SD of Tb.Th against the mean, mode and mineral heterogeneity of the BMDD curves in the OVX group at day 0 and week 4, 8, 14 and 34 (OVX n = 5)
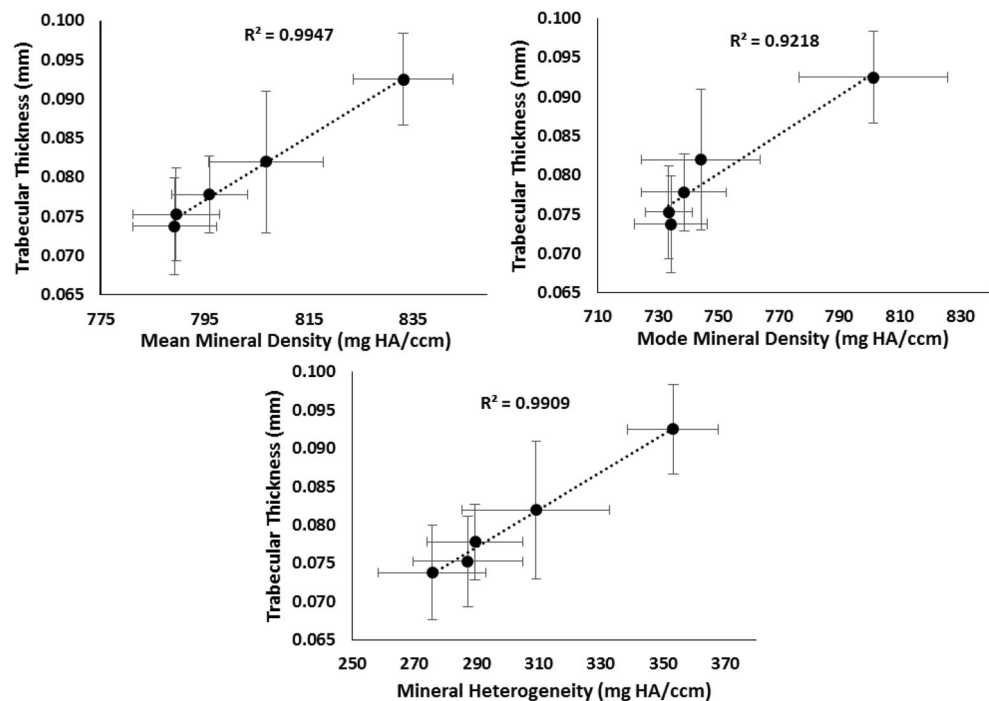
rat is well-established model, due to similarities with respect to bone loss [22–24], an initial period of rapid bone loss followed by a return to a more balanced remodelling process as bone loss reaches a plateau [21], calcium absorption [22, 25, 26] and skeletal responses to drug treatments and exercise [27–30], which are all characteristic of human postmenopausal osteoporosis. At the beginning of this study, the predominant bone metabolic activity in the proximal tibial metaphysis of the 6-month old rats is transitioning from bone modelling to bone remodelling, which continues until 9 months old [21]. However, only the OVX animals demonstrate early bone loss followed by an altered mineral distribution, whereas the controls did not. Furthermore, an in vivo μCT analysis of the proximal tibial metaphysis in 10-month old rats, which should have finished modelling [8], also observed early bone loss in OVX animals, followed by a decreased rate of bone loss and an increased mean trabecular thickness in long-term estrogen deficiency. Secondly, there were some differences between OVX and SHAM animals at the baseline (day 0) with regard to the microarchitecture parameters (SMI, DA) for the initial phase study and mineralisation (low mineral BV, high mineral BV) for the long-term study. This variability might be due to biological variations, arising from the animal weight (greater in SHAM than OVX for animals in the long-term study) or the number of breeding cycles prior to retirement, which was unknown and likely varied, both of which are correlated to trabecular bone structure [31]. It is important to note that SMI and DA are only indicators of the average shape (calculated under the generalised assumption that all bone surfaces are concave [32]) and alignment of the trabecular structure, respectively, whereas BV/TV, Tb.Sp and Tb.N are widely used to understand bone loss dynamics. These parameters (BV/TV, Tb.Sp and Tb.N) were not significantly different at the baseline, and the OVX animals demonstrated rapid and early bone loss, and indeed they were significantly different to Sham by week 1 (reduced BV/TV), week 3 (increased Tb.Sp) and week 4 (reduced Tb.N), followed by an altered bone mineral distribution, whereas the controls did not. The surface voxels (one layer) from every trabecula were excluded from BMDD analysis, to reduce partial volume effects. This would remove 30 μm of the width (2 × 15 μm voxels) of each trabecula and may exclude trabeculae with a thickness less than 45 μm from BMDD analysis. Nonetheless, despite the exclusion of these surface voxels, we have captured important mineralisation changes during long-term estrogen deficiency, which have not been previously reported.

Previous studies have used micro-CT and traditional histomorphometry to study bone loss in trabecular in estrogen deficiency [3–5]. A significant reduction in bone volume fraction within the first 4 weeks of ovariectomy surgery has been reported in vivo [6–9], and bone loss and trabecular thickening at the late stages of estrogen deficiency have also been previously reported (week 8 [6], 14 [8] and 16 [7]). Our results

showing an increase in trabecular thickness after 14 weeks provide further validation of the theory that proposed that this arises due to a compensatory response at later stages of estrogen deficiency [8], to reinforce the remaining bone structure and strength after severe bone loss. The period of rapid bone loss during the second week after surgery we report here may be driven by an accelerated bone metabolism that is triggered by estrogen depletion [31]. Perhaps the trabeculae lost during this initial phase are not essential for load bearing in their particular alignment and are regarded as dispensable during the state of accelerated bone metabolism that occurs in estrogen deficiency. We do not believe that this bone loss is driven by trabecular thinning alone, leading to selective loss of the thinner structures, as we would expect this to lead to an increased group mean or reduced standard deviation in trabecular thickness, during the initial resorptive phase of estrogen deficiency, which we did not observe. Furthermore, trabecular thinning should predominantly remove lower mineralised tissue from the trabecular surface; however this study indicates tissue from all levels of mineralisation was removed during the initial phase of bone loss. Thus bone loss is likely a combination of variable thinning and perforation of trabeculae, rather than uniform thinning along the entire surface of the trabecula. We report that rapid loss of trabeculae concludes after the 14th week of estrogen deficiency, which might be a sign of acclimatisation to the estrogen-deficient conditions and a return to a normal bone resorption rate. Studies of the ovariectomised rat have observed an initial period of rapid bone loss immediately after ovariectomy, which is followed by a return to a more balanced remodelling process as bone loss reaches a plateau [6–9]. This renewed homeostasis of bone remodelling may be contributed to by thickening of trabeculae from week 14 of estrogen deficiency, which together indicate that the depleted structure is being reinforced to adapt to an altered load distribution subsequent to severe bone loss.

We report here for the first time that there is an increase in the heterogeneity of the mineral distribution, which occurs in the longer term of estrogen deficiency and does not coincide with the initial phase of rapid bone loss. Previous studies of bone mineralisation in estrogen-deficient rat models have reported conflicting results, whereby qBEI analysis reported no difference between OVX and age-matched controls with respect to mean mineral density in the vertebrae and femur at 12 weeks, 48 weeks [14] and 20.5 months [15], whereas a minimal reduction of mineral heterogeneity at 20.5 months of estrogen deficiency [15]. However, qBEI provides only a 2D assessment of bone mineralisation and thus may have not fully captured changes arising in the bone. Using ex-vivo micro-CT and SRμCT (3D), it was reported that there was no difference in mean mineral density in the lumbar vertebrae and tibia of OVX rats compared to age-matched controls at 14 [32], 16 or 32 weeks [16] or mode mineral density or mineral heterogeneity at 14 weeks [32]. In contrast to each of these studies

[14–16, 32], we report that the mean mineral density and mineral heterogeneity were increased by week 14 in estrogen-deficient animals, compared to their baseline, and this continues to increase further until week 34 and occurs at a much faster rate than mineralisation observed in normal ageing. The differences may be due to the difference in age of the animal models, breed, reproductive history, biological variation between unique animal groups or anatomical location for assessment. Moreover, a site-specific alteration of mineral distribution was previously seen in ovariectomised sheep [11]. However, in contrast to a previous study [16] that reported a higher percentage of low mineral content bone tissue after 16 and 32 weeks of estrogen deficiency (compared to age-matched controls), we report that the proportion of bone at low mineral density was decreasing, while that at high mineral density was increasing between week 8 and week 34 in OVX animals. To our knowledge, the results we report in this study provide the first in vivo study of bone mineral distribution in a rat model during the first 4 weeks of estrogen deficiency, indicating that structural changes arise prior to changes in bone tissue composition and that these do not coincide with the initial phase of rapid bone loss. We have also shown for the first time in vivo that the mean mineral density and mineral heterogeneity in the tibia of an estrogen-deficient rat model are significantly increased in long-term estrogen deficiency.

The increased mineralisation in longer-term estrogen deficiency may be due to natural maturation and may be partly contributed to by micropetrosis, as it is known there are higher rates of osteocyte apoptosis in estrogen deficiency [33, 34]. However, we previously reported that the mechanical environment of osteoblasts and osteocytes is altered in the initial phase of estrogen deficiency, but that the mechanical environment of the cells was restored to normal levels in long-term estrogen deficiency [17]. Thus, we propose that the changes in mineralisation seen here may arise in response to this altered cellular mechanical environment following early bone loss. It has been previously reported that collagen synthesis is increased in osteoporosis [35, 36]. This may result in a change in quality of collagen fibrils and formation of smaller diameter fibrils [37]. This increase in collagen synthesis may be happening gradually during this initial phase of estrogen deficiency, and since collagen acts as a scaffold for bone minerals, alterations of the collagen framework are likely to be contributing to the altered tissue mineralisation which we observed in long-term estrogen deficiency. The heterogeneity in the tissue may be contributed to by hyper mineralisation of existing tissue and also the formation of new bone tissue at the surface of thickening trabeculae. Indeed, the increased trabecular thickness observed in our study was significantly correlated to the altered mineralisation (Fig. 6). Furthermore, in late stages of estrogen deficiency, when bone loss has reached a plateau, there is a reduction in the amount of lower mineralised tissue and an increase in the amount of highly mineralised tissue present, which suggests hyper mineralisation of the existing tissue is contributing to the increase in mineral heterogeneity and mean mineral density.

The results presented here provide an advanced understanding of the temporal changes in bone mineral distribution during estrogen deficiency in a rat model. We propose that the depleted trabecular structure remaining after the initial phase of rapid bone loss is reinforced (by means of mineralisation and trabecular thickening) in longer-term estrogen deficiency in an attempt to maintain strength in the remaining tissue. Although it has been reported that mineralisation was altered in trabecular tissue from human osteoporosis [10], whether this occurs secondary to bone loss is unknown. Further investigations should be carried out to establish the temporal nature of alterations to mineral distribution in human osteoporosis.

Conclusion

In summary, although trabecular bone volume and architecture deteriorate within the first 4 weeks of estrogen deficiency, there is no immediate change in the distribution of mineral within trabeculae in this period. However, in longer-term estrogen deficiency, there is a reinforcement of the remaining trabeculae, through both mineralisation of existing tissue and formation of new bone on the remaining trabecular surfaces, and we propose that this arises in response to the altered loading conditions in the deteriorated structure after bone loss has occurred.

Compliance with ethical standards

Conflicts of interest None.

References

1. Parfitt AM (1987) Trabecular bone architecture in the pathogenesis and prevention of fracture. Am J Med 82:68–72
2. Compston JE, Mellish RWE, Croucher P, Newcombe R, Garrahan NJ (1989) Structural mechanisms of trabecular bone loss in man. Bone Miner 6:339–350. https://doi.org/10.1016/0169-6009(89)90039-1
3. Lane NE, Thompson JM, Haupt D, Kimmel DB, Modin G, Kinney JH (1998) Acute changes in trabecular bone connectivity and osteoclast activity in the ovariectomized rat in vivo. J Bone Miner Res 13:229–236. https://doi.org/10.1359/jbmr.1998.13.2.229
4. Laib A, Kumer JL, Majumdar S, Lane NE (2001) The temporal changes of trabecular architecture in ovariectomized rats assessed

by micro-CT. Osteoporos Int 12:936–941. https://doi.org/10.1007/s001980170022

5. Dempster DW, Birchman R, Xu R, Lindsay R, Shen V (1995) Temporal changes in cancellous bone structure of rats immediately after ovariectomy. Bone 16:157–161. https://doi.org/10.1016/8756-3282(95)80027-N

6. Perilli E, Le V, Ma B et al (2010) Detecting early bone changes using in vivo micro-CT in ovariectomized, zoledronic acid-treated, and sham-operated rats. Osteoporos Int 21:1371–1382. https://doi.org/10.1007/s00198-009-1082-z

7. Brouwers JEM, Lambers FM, Gasser JA et al (2008) Bone degeneration and recovery after early and late bisphosphonate treatment of ovariectomized Wistar rats assessed by in vivo micro-computed tomography. Calcif Tissue Int 82:202–211. https://doi.org/10.1007/s00223-007-9084-3

8. Waarsing JH, Day JS, Verhaar JAN, Ederveen AG, Weinans H (2006) Bone loss dynamics result in trabecular alignment in aging and ovariectomized rats. J Orthop Res 24:926–935. https://doi.org/10.1002/jor.20063

9. Boyd SK, Davison P, Müller R, Gasser JA (2006) Monitoring individual morphological changes over time in ovariectomized rats by in vivo micro-computed tomography. Bone 39:854–862. https://doi.org/10.1016/j.bone.2006.04.017

10. Busse B, Hahn M, Soltau M et al (2009) Increased calcium content and inhomogeneity of mineralization render bone toughness in osteoporosis: mineralization, morphology and biomechanics of human single trabeculae. Bone 45:1034–1043. https://doi.org/10.1016/j.bone.2009.08.002

11. Brennan M, Gleeson J, Browne M et al (2011) Site specific increase in heterogeneity of trabecular bone tissue mineral during oestrogen deficiency. Eur Cells Mater 21:396–406. https://doi.org/10.22203/eCM.v021a30

12. Brennan O, Kuliwaba JS, Lee TC, Parkinson IH, Fazzalari NL, McNamara L, O'Brien FJ (2012) Temporal changes in bone composition, architecture, and strength following estrogen deficiency in osteoporosis. Calcif Tissue Int 91:440–449. https://doi.org/10.1007/s00223-012-9657-7

13. Brennan MA, Gleeson JP, O'Brien FJ, McNamara LM (2014) Effects of ageing, prolonged estrogen deficiency and zoledronate on bone tissue mineral distribution. J Mech Behav Biomed Mater 29:161–170. https://doi.org/10.1016/j.jmbbm.2013.08.029

14. Kneissel M, Boyde A, Gasser J (2001) Bone tissue and its mineralization in aged estrogen-depleted rats after long-term intermittent treatment with parathyroid hormone (PTH) analog SDZ PTS 893 or human PTH(1-34). Bone 28:237–250. https://doi.org/10.1016/S8756-3282(00)00448-8

15. Valenta A, Roschger P, Fratzl-Zelman N, Kostenuik PJ, Dunstan CR, Fratzl P, Klaushofer K (2005) Combined treatment with PTH (1–34) and OPG increases bone volume and uniformity of mineralization in aged ovariectomized rats. Bone 37:87–95. https://doi.org/10.1016/J.BONE.2005.03.013

16. Cheng Z, Yao W, Zimmermann EA, Busse C, Ritchie RO, Lane NE (2009) Prolonged treatments with antiresorptive agents and PTH have different effects on bone strength and the degree of mineralization in old estrogen-deficient osteoporotic rats. J Bone Miner Res 24:209–220. https://doi.org/10.1359/jbmr.81005

17. Verbruggen SW, Mc Garrigle MJ, Haugh MG et al (2015) Altered mechanical environment of bone cells in an animal model of short- and long-term osteoporosis. Biophys J 108:1587–1598. https://doi.org/10.1016/j.bpj.2015.02.031

18. Brouwers JEM, van Rietbergen B, Huiskes R (2007) No effects of in vivo micro-CT radiation on structural parameters and bone marrow cells in proximal tibia of Wistar rats detected after eight weekly scans. J Orthop Res 25:1325–1332. https://doi.org/10.1002/jor.20439

19. Bouxsein ML, Boyd SK, Christiansen BA et al (2010) Guidelines for assessment of bone microstructure in rodents using micro-computed tomography. J Bone Miner Res 25:1468–1486. https://doi.org/10.1002/jbmr.141

20. Roschger P, Paschalis EP, Fratzl P, Klaushofer K (2008) Bone mineralization density distribution in health and disease. Bone 42:456–466. https://doi.org/10.1016/j.bone.2007.10.021

21. Lelovas PP, Xanthos TT, Thoma SE, Lyritis GP, Dontas IA (2008) The laboratory rat as an animal model for osteoporosis research. Comp Med 58:424–430

22. Kalu DN (1991) The ovariectomized rat model of postmenopausal bone loss. Bone Miner 15:175–191. https://doi.org/10.1016/0169-6009(91)90124-I

23. Štěpán JJ, Musilová J, Pacovský V (2009) Bone demineralization, biochemical indices of bone remodeling, and estrogen replacement therapy in adults with Turner's syndrome. J Bone Miner Res 4:193–198. https://doi.org/10.1002/jbmr.5650040210

24. Gallagher JC (1990) The pathogenesis of osteoporosis. Bone Miner 9:215–227. https://doi.org/10.1016/0169-6009(90)90039-I

25. Gallagher JC, Riggs BL, Eisman J, Hamstra A, Arnaud SB, DeLuca H (1979) Intestinal calcium absorption and serum vitamin D metabolites in normal subjects and osteoporotic patients. J Clin Invest 64:729–736. https://doi.org/10.1172/JCI109516

26. Heaney RP, Recker RR, Omaha PDS (2009) Menopausal changes in calcium balance performance. Nutr Rev 41:86–89. https://doi.org/10.1111/j.1753-4887.1983.tb07709.x

27. Reeve J, Meunier PJ, Parsons JA et al (1980) Anabolic effect of human parathyroid hormone fragment on trabecular bone in involutional osteoporosis: a multicentre trial. BMJ 280:1340–1344. https://doi.org/10.1136/bmj.280.6228.1340

28. Wronski TJ, Dann LM, Scott KS, Crooke LR (1989) Endocrine and pharmacological suppressors of bone turnover protect against osteopenia in ovariectomized rats. Endocrinology 125:810–816. https://doi.org/10.1210/endo-125-2-810

29. WronskiI TJ, Cintron M, Doherty AL, Dann LM (1988) Estrogen treatment prevents osteopenia and depresses bone turnover in ovariectomized rats. Endocrinology 123:681–686. https://doi.org/10.1210/endo-123-2-681

30. Simkin A, Ayalon J, Leichter I (1987) Increased trabecular bone density due to bone-loading exercises in postmenopausal osteoporotic women. Calcif Tissue Int 40:59–63. https://doi.org/10.1007/BF02555706

31. Thompson DD, Simmons HA, Pirie CM, Ke HZ (1995) FDA guidelines and animal models for osteoporosis. Bone 17:S125–S133. https://doi.org/10.1016/8756-3282(95)00285-L

32. Campbell GM, Bernhardt R, Scharnweber D, Boyd SK (2011) The bone architecture is enhanced with combined PTH and alendronate treatment compared to monotherapy while maintaining the state of surface mineralization in the OVX rat. Bone 49:225–232. https://doi.org/10.1016/j.bone.2011.04.008

33. Kousteni S, Bellido T, Plotkin LI, O'Brien CA, Bodenner DL, Han L, Han K, DiGregorio G, Katzenellenbogen JA, Katzenellenbogen BS, Roberson PK, Weinstein RS, Jilka RL, Manolagas SC (2001) Nongenotropic, sex-nonspecific signaling through the estrogen or androgen receptors. Cell 104:719–730. https://doi.org/10.1016/S0092-8674(01)00268-9

34. Tomkinson A (1997) The death of osteocytes via apoptosis accompanies estrogen withdrawal in human bone. J Clin Endocrinol Metab 82:3128–3135. https://doi.org/10.1210/jc.82.9.3128

35. Bailey AJ, Wotton SF, Sims TJ, Thompson PW (1993) Biochemical changes in the collagen of human osteoporotic bone matrix. Connect Tissue Res 29:119–132. https://doi.org/10.3109/03008209309014239

36. Mansell J, Bailey A (2003) Increased metabolism of bone collagen in post-menopausal female osteoporotic femoral heads. Int J Biochem Cell Biol 35:522–529. https://doi.org/10.1016/S1357-2725(02)00312-6

37. Viguet-Carrin S, Garnero P, Delmas PD (2006) The role of collagen in bone strength. Osteoporos Int 17:319–336. https://doi.org/10.1007/s00198-005-2035-9